Molecular dynamics study of a dipolar fluid between charged plates. II

Song Hi Lee[a] and Jayendran C. Rasaiah
Department of Chemistry, University of Maine, Orono, Maine 04469

J. B. Hubbard
Thermophysics Division, National Bureau of Standards, Gaithersburg, Maryland 20899

(Received 13 August 1986; accepted 23 October 1986)

Further molecular dynamics simulations of thin films of Stockmayer molecules between Lennard-Jones plates are discussed when the distance h between the plates ranges from 2.25 σ to 9.5 σ, where σ is the molecular diameter, and the electric field $\mathbf{E}$ ranges between 0 and 10^{10} V/m. The solvation force is calculated as a function of the plate separation h when $\mathbf{E} = 0$ and $\mathbf{E} = 10^9$ V/m and as a function of the field $\mathbf{E}$ when $h = 4.0\,\sigma$ and 7.5 σ. We also study the system when $h = 2.25\,\sigma$ and 4.0 σ with the field $\mathbf{E}$ ranging from 0 to 10^{10} V/m and find that the monolayer system ($h = 2.25\,\sigma$) seems to undergo changes of state as the temperature is lowered at zero field or if the field is changed at low temperature. While, in the absence of a field, the molecules tend to form loops and chain-like structures with the dipoles parallel to the wall, a strong external field orients the dipoles along the field so that the long-range repulsive interaction appears to induce a transition to an imperfect (two-dimensional) triangular lattice at low temperature. In between these states, at low temperatures and high fields, the molecules are packed in parallel chains with their moments perpendicular to the field and in "ferroelectric domains" of opposite polarization.

I. INTRODUCTION

In a previous communication,[1] we discussed a molecular dynamics study of a thin film of Stockmayer molecules between Lennard-Jones plates separated by a distance $h = 7.5\,\sigma$, where σ is the Lennard-Jones diameter. These studies were carried out in the presence of an electric field $\mathbf{E}$ between the plates and in its absence. Our attention was mainly confined to the density and polarization density profiles, to the components of the total dipole moment parallel and perpendicular to the walls, and to the decay of the dipole autocorrelation functions. Continuing that study here, we discuss new results at smaller ($h = 2.25\,\sigma$, 3.2 σ, and 4.0 σ) and larger ($h = 9.5\,\sigma$) plate separations which include the solvation force as a function of h when $\mathbf{E} = 0$ and $\mathbf{E} = 10^9$ V/m and as a function of $\mathbf{E}$ when the plate separations are 4.0 σ and 7.5 σ, respectively. We have also extended our earlier investigations[1] of the polarization density profiles as a function of the electric field to different plate separations and confirm our previous observation[1] that the dipoles in the first layers near the plates are mostly oriented parallel to the surface in the absence of a field between the plates, and that the polarization density $\langle P_z(z,\mathbf{E})\rangle$, in the direction of the field, is fairly well approximated by the product of local density $\langle \rho(z)\rangle$ and the component of the dipole moment $\langle \mu_z(z)\rangle$ parallel to the field. Our study of a monolayer film between plates separated by 2.25 σ reveals unusual features that accompany the freezing of the rotational and translational motion of dipoles in this layer when the temperature is lowered. This has lead us to a detailed examination of the equilibrium and dynamic properties of this system in fields up to $\mathbf{E} = 10^{10}$ V/m providing an interesting account of the changes brought about by a reduction in dimensionality.

A theoretical and computer simulation study of the force between two parallel plates immersed in a fluid of hard spheres has been carried out recently by Wertheim, Blum, and Bratkos.[2(a)] For very small gaps, barely exceeding one sphere diameter σ, they derived the exact limiting law that the density approaches the fugacity as the gap width approaches σ. They also compared their theoretical predictions of the density profiles with the simulations. Monte Carlo simulations of this system have also been performed by Snook and Henderson.[2(b)] A molecular dynamics simulation of atomic self-diffusion in a thin film of Lennard-Jones molecules has been carried out recently[3] where it is found that the time needed for diffusive behavior to show up increases substantially for thinner systems, thereby signifying the lack of diffusion in a two-dimensional system. Earlier simulations that are most closely related to our work are the Monte-Carlo and molecular dynamics calculations of Snook and van Megan[4] and Magda *et al.*,[5] respectively, who studied Lennard-Jones molecules between Lennard-Jones walls. However, our study is, as far as we know, the first detailed investigation of the solvation force and dynamics of a simple polar fluid between plates in the presence of a strong electric field. Theories of the solvation force between plates have been reviewed by Rickayzen.[6]

In Sec. II we present some details of the molecular dynamics simulation in addition to those discussed briefly in Sec. II of our previous paper[1]; our results and conclusions are discussed in Sec. III.

II. DETAILS OF THE MOLECULAR DYNAMICS SIMULATION

The pair potential for a Stockmayer fluid[7] is given by

$$u_{ij}(\mathbf{r},\boldsymbol{\mu}_i,\boldsymbol{\mu}_j) = 4\epsilon[(\sigma/r)^{12} - (\sigma/r)^6] - \boldsymbol{\mu}_i\cdot\mathbf{T}\cdot\boldsymbol{\mu}_j\,, \qquad (2.1)$$

where $\mathbf{r} = \mathbf{r}_i - \mathbf{r}_j$, $r = |\mathbf{r}|$, $\boldsymbol{\mu}_i$ is the dipole moment vector of particle i, ϵ and σ are the Lennard-Jones parameters, and $\mathbf{T}$ is

[a] Present address: Department of Chemistry, University of Texas at Austin, TX 78712.

 0021-9606/87/042383-11$02.10

the dipole interaction tensor

$$\mathbf{T} = (3\mathbf{rr}/r^2 - \mathbf{U})/r^3 \tag{2.2}$$

where U is the unit matrix. The dipole–dipole potential energy, force, and torque for particle i in the absence of an external field without Ewald summation are given in Ref. 1. The corresponding equations with Ewald summation are, however, much more complicated. Each equation splits into the sum of two parts, one in real space and the other in reciprocal space.[8] The effective dipole–dipole potential for a periodic system, surrounded by a vacuum, can be written as

$$U_{DD} = -(1/L)(\boldsymbol{\mu}_i\cdot\nabla)(\boldsymbol{\mu}_i\cdot\nabla)\Psi(\mathbf{r}/L)\,, \tag{2.3}$$

where L is the length of the side of the cubic simulation sample that contains N particles and the function $\Psi(\mathbf{r})$ is given by

$$\Psi(\mathbf{r}) = \sum_{\mathbf{n}} \operatorname{erfc}(\alpha|\mathbf{r}+\mathbf{n}|)/|\mathbf{r}+\mathbf{n}| \quad \text{:real space} \tag{2.4a}$$

$$+ (1/\pi)\sum_{\mathbf{n}\neq 0} |\mathbf{n}|^{-2}\exp[2\pi i\mathbf{n}\cdot\mathbf{r} - \pi^2|\mathbf{n}|^2/\alpha^2] \quad \text{:reciprocal space} \tag{2.4b}$$

in which

$$\operatorname{erfc}(x) = 1 - 2\pi^{-1/2}\int_0^x \exp(-t^2)dt \tag{2.5}$$

is the complementary error function. The parameter α and the integer coordinates $\mathbf{n} = (l,m,n)$ are chosen in such a way that a high accuracy of calculation is combined with a minimum of computing work. In real space we consider only $\mathbf{n} = (0,0,0)$ since the contribution of the other n's are vanishingly small. Then the dipole–dipole potential energy, force, and torque are, for particle i in the absence of an external field, given by

$$U^{\text{real}}_{DD,i} = (1/L^3)\sum_{j\neq i}\{(\boldsymbol{\mu}_i\cdot\boldsymbol{\mu}_j)[2\pi^{-1/2}\alpha\exp(-\alpha^2|\mathbf{r}/L|^2)/|\mathbf{r}/L|^2 + \operatorname{erfc}(\alpha|\mathbf{r}/L|)/|\mathbf{r}/L|^3]$$
$$- (\boldsymbol{\mu}_i\cdot\mathbf{r}/L)(\boldsymbol{\mu}_j\cdot\mathbf{r}/L)[4\pi^{-1/2}\alpha^3\exp(-\alpha^2|\mathbf{r}/L|^2)/|\mathbf{r}/L|^2$$
$$+ 6\pi^{-1/2}\alpha\exp(-\alpha^2|\mathbf{r}/L|^2)/|\mathbf{r}/L|^4 + 3\operatorname{erfc}(\alpha|\mathbf{r}/L|)/|\mathbf{r}/L|^5]\}\,, \tag{2.6a}$$

$$\mathbf{F}^{\text{real}}_{DD,i} = (1/L^3)\sum_{j\neq i}\{[(\boldsymbol{\mu}_i\cdot\boldsymbol{\mu}_j)\mathbf{r}/L + \boldsymbol{\mu}_i(\boldsymbol{\mu}_j\cdot\mathbf{r}/L) + \boldsymbol{\mu}_j(\boldsymbol{\mu}_i\cdot\mathbf{r}/L)]$$
$$\times[4\pi^{-1/2}\alpha^3\exp(-\alpha^2|\mathbf{r}/L|^2)/|\mathbf{r}/L|^2 + 6\pi^{-1/2}\alpha\exp(-\alpha^2|\mathbf{r}/L|^2)/|\mathbf{r}/L|^4 + 3\operatorname{erfc}(\alpha|\mathbf{r}/L|)/|\mathbf{r}/L|^5]$$
$$- (\boldsymbol{\mu}_i\cdot\mathbf{r}/L)(\boldsymbol{\mu}_j\cdot\mathbf{r}/L)\mathbf{r}/L\,[8\pi^{-1/2}\alpha^5\exp(-\alpha^2|\mathbf{r}/L|^2)/|\mathbf{r}/L|^2$$
$$+ 20\pi^{-1/2}\alpha^3\exp(-\alpha^2|\mathbf{r}/L|^2)/|\mathbf{r}/L| + 30\pi^{-1/2}\alpha^2\exp(-\alpha^2|\mathbf{r}/L|^2)/|\mathbf{r}/L|^6$$
$$+ 15\operatorname{erfc}(\alpha|\mathbf{r}/L|)/|\mathbf{r}/L|^7]\}\,, \tag{2.6b}$$

$$\mathbf{T}^{\text{real}}_{DD,i} = (1/L^3)\sum_{j\neq i}\{-\boldsymbol{\mu}_j[2\pi^{-1/2}\alpha\exp(-\alpha^2|\mathbf{r}/L|^2)/|\mathbf{r}/L|^2 + \operatorname{erfc}(\alpha|\mathbf{r}/L|)/|\mathbf{r}/L|^3]$$
$$+ (\boldsymbol{\mu}_j\cdot\mathbf{r}/L)\mathbf{r}/L\,[4\pi^{-1/2}\alpha^3\exp(-\alpha^2|\mathbf{r}/L|^2)/|\mathbf{r}/L|^2$$
$$+ 6\pi^{-1/2}\alpha\exp(-\alpha^2|\mathbf{r}/L|^2)/|\mathbf{r}/L|^4 + 3\operatorname{erfc}(\alpha|\mathbf{r}/L|)/|\mathbf{r}/L|^5]\}\,. \tag{2.6c}$$

Letting $\alpha = 0$ in Eqs. (2.6), we recover the equations without the Ewald summation, i.e., Eqs. (2.4) of Ref. 1. Substituting Eq. (2.4b) into Eq. (2.3) and summing over particles i and j, we obtain the total dipole–dipole potential energy in the reciprocal space:

$$U^{rcpr}_{DD}(\text{total}) = (2\pi/L^3)\sum_{\mathbf{n}\neq 0} f(\mathbf{n})\sum_{i\neq j}\sum_j (\boldsymbol{\mu}_i\cdot\mathbf{n})(\boldsymbol{\mu}_j\cdot\mathbf{n})$$
$$\times\exp(2\pi i\mathbf{n}\cdot\mathbf{r}/L)\,,$$

where $f(\mathbf{n}) = \exp(-\pi^2|\mathbf{n}|^2\alpha^2)/|\mathbf{n}|^2$. This equation can be simplified considerably by using the identity

$$\sum_{i\neq j}\sum_j (\boldsymbol{\mu}_i\cdot\mathbf{n})(\boldsymbol{\mu}_j\cdot\mathbf{n})\exp(2\pi i\mathbf{n}\cdot\mathbf{r}/L)$$
$$= \sum_i (\boldsymbol{\mu}_i\cdot\mathbf{n})\exp(2\pi i\mathbf{n}\cdot\mathbf{r}_i/L)\sum_j (\boldsymbol{\mu}_j\cdot\mathbf{n})$$
$$\times\exp(-2\pi i\mathbf{n}\cdot\mathbf{r}_j/L) - \sum_i (\boldsymbol{\mu}_i\cdot\mathbf{n})^2$$
$$= |S(\mathbf{n})|^2 - T(\mathbf{n})\,, \tag{2.7}$$

where

$$S(\mathbf{n}) = \sum_i (\boldsymbol{\mu}_i\cdot\mathbf{n})\exp(-2\pi i\mathbf{n}\cdot\mathbf{r}_i/L)\,, \tag{2.8a}$$

$$T(\mathbf{n}) = \sum_i (\boldsymbol{\mu}_i\cdot\mathbf{n})^2\,. \tag{2.8b}$$

Hence,

$$U^{rcpr}_{DD}(\text{total}) = (2\pi/L^3)\sum_{\mathbf{n}\neq 0} f(\mathbf{n})[|S(\mathbf{n})|^2 - T(\mathbf{n})]\,. \tag{2.9a}$$

This trick, first suggested by Woodcock and Singer,[9] reduces the computing time by a factor of the order of the number of particles in the system. The dipole–dipole force and torque for particle i in reciprocal space are obtained by applying the same trick:

$$\mathbf{F}^{rcpr}_{DD} = (8\pi^2/L^4)\sum_{\mathbf{n}\neq 0} f(\mathbf{n})\mathbf{n}i(\boldsymbol{\mu}_i\cdot\mathbf{n})[S(\mathbf{n})$$

$$\times\exp(2\pi i\mathbf{n}\cdot\mathbf{r}_i/L) - (\boldsymbol{\mu}_i\cdot\mathbf{n})]\,, \tag{2.9b}$$

$$\mathbf{T}_{DD}^{rcpr} = -(4\pi/L^3)\sum_{\mathbf{n}\neq 0} f(\mathbf{n})\mathbf{n}[S(\mathbf{n})$$

$$\times\exp(2\pi i\mathbf{n}\cdot\mathbf{r}_i/L) - (\boldsymbol{\mu}_i\cdot\mathbf{n})]\,. \tag{2.9c}$$

Letting $\alpha = 0$ in $f(\mathbf{n})$ makes $f(\mathbf{n}) = 0$ leaving the terms in reciprocal space equal to zero.

The interaction between the fluid particles and the infinite Lennard-Jones walls placed at distances equal to $+\sigma$ and $-\sigma$ from the x–y planes of the rectangular box is given by[4]

$$u_w(z) = 2\pi\epsilon[0.4(\sigma/z)^{10} - (\sigma/z)^4 - (\sqrt{2}/3)(z/\sigma + 0.61/\sqrt{2})^{-3}] \tag{2.10}$$

and the wall–particle force is derived as

$$\mathbf{F}_w(\mathbf{z}) = 8\pi\epsilon\mathbf{z}[(\sigma/z)^{10} - (\sigma/z)^4 - (\sqrt{2}z/4\sigma)(z/\sigma + 0.61/\sqrt{2})^{-4}]/z^2 \tag{2.11}$$

Since there are two such walls, the Lennard-Jones wall–dipole interaction for particle i is given by

$$U_{w,i}(z_i) = u_w(z_i - z_1) + u_w(z_i - z_2)\,, \tag{2.12}$$

$$\mathbf{F}_{w,i}(z_i) = \mathbf{F}_w(z_i - z_1) + \mathbf{F}_w(z_i - z_2)\,, \tag{2.13}$$

where z_1 and z_2 are the locations of the two walls. By definition the solvation force is the time-averaged force per unit area exerted by all the particles upon each Lennard-Jones wall[4,5]:

$$f_s = -(1/2A)\left\langle \sum_i \frac{dU_w(z_i)}{dz_i} + \frac{dU_w(h - z_i)}{dz_i}\right\rangle, \tag{2.14a}$$

where A is the area of the wall and U_w is the interaction potential between particle and wall. Another expression for the solvation force due to Irving and Kirkwood[10] is

$$f_s = NkT/hA - (1/hA)\left\langle \sum_{i,j} z_{ij}\frac{dU_T(dr_{ij})}{r_{ij}}dr_{ij} + \sum_i\left[z_i\frac{dU_w(z_i)}{dz_i} + (h - z_i)\frac{dU_w(h - z_i)}{dz_i}\right]\right\rangle, \tag{2.14b}$$

where $z_{ij} = z_i - z_j$, $r_{ij} = |\mathbf{r}_i - \mathbf{r}_j|$ and U_T represents the total interaction potential between particles i and j.

The simulation was carried out in rectangular boxes of dimensions $7\times7\times h\sigma^3$ where h/σ and the number of particles N are set equal to 2.25 (38), 2.5 (41), 2.75 (63), 3.0 (71), 3.2 (73), 3.5 (78), 3.75 (95), 4.0 (103), 7.5 (206), and 9.5 (264), respectively, for the several systems studied by us. The equations of motion are obtained from the Lagrangian

$$L = \sum_i \frac{1}{2}mv_i^2 + (1/\mu^2)\sum_i \frac{1}{2}\mathbf{I}\dot{\mu}_i^2 + \frac{1}{2}\sum_{i\neq j}\sum_j \boldsymbol{\mu}_i\cdot\mathbf{T}\cdot\boldsymbol{\mu}_j - \frac{1}{2}\sum_i\sum_j u_{ij}^{LJ} + \sum_i \lambda_i(\mu_i^2 - \mu^2) + \sum_i \boldsymbol{\mu}_i\cdot\mathbf{E}\,. \tag{2.15}$$

The first two terms are the translational and rotational kinetic energies, respectively, and the third and fourth terms represent the dipole–dipole and Lennard-Jones interaction energies. We use the method of constraints introduced by Ryckaert *et al.*[12] and adapted by Pollack and Alder[13] to Stockmayer fluids to treat the rotational part of the motion. Thus the fifth term in the Lagrangian contains the constraint variables which enable the components of $\boldsymbol{\mu}$ to be treated in Cartesian rather than spherical polar cordinates by the introduction of Lagrangian multipliers λ_i such that $\mu^2 = |\boldsymbol{\mu}_i|^2$ at all times. The last term in the Lagrangian comes from the interaction of the dipoles with the external field.

The equation of motion for the translational degree of freedom is

$$m\ddot{\mathbf{r}}_i = \boldsymbol{\mu}_i\cdot\sum_{j\neq i}\nabla\mathbf{T}\cdot\boldsymbol{\mu}_j + \boldsymbol{\mu}_i\cdot\nabla\mathbf{E} + \mathbf{F}_i^{LJ}\,, \tag{2.16}$$

in which the last term is the Lennard-Jones force and $\nabla\mathbf{E}$ is zero in our systems. The corresponding equation for the rotational degree of freedom is

$$(1/\mu^2)\ddot{\boldsymbol{\mu}}_i = \sum_{j\neq i}\mathbf{T}\cdot\boldsymbol{\mu}_j + \mathbf{E} + 2\lambda_i\boldsymbol{\mu}_i \tag{2.17}$$

which contains the Lagrangian multiplier λ_i. Pollack and Alder[13] used the Verlet algorithm to integrate their equations of motion; the variable λ_i was determined by solving a quadratic equation arising from the condition that the magnitude of the dipole moment was a constant at every time step. Instead we use the leapfrog algorithm[14] which requires a different value of λ_i to maintain this constancy; the details of this calculation are provided in an appendix. The other simulation parameters are the same as those used in our previous study.[1] The mass of each particle was taken as 6.63×10^{-26} kg and the mean reduced density $\rho^* = \rho\sigma^3$ was 0.5605. The reduced temperature ($T^* = kT/\epsilon$) was maintained at 1.18 (i.e., $T = 148$ K) except for a monolayer film which was studied at temperatures ranging from 148 to 5 K. The particles were endowed with a moment of inertia equal to $0.025m\sigma^2$ and a time step of 5 fs was used for the rotational

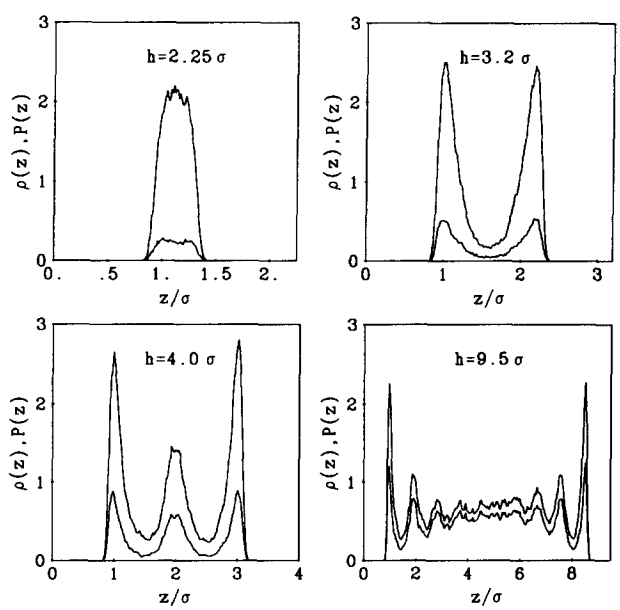

FIG. 1. The density and polarization profiles for a Stockmayer fluid between plates separated at distances h of 2.25, 3.2, 4.0 and 9.5 σ in the presence of an electric field $\mathbf{E} = 10^9$ V/m between the plates. The actual density and polarization are obtained by multiplying $\rho(z)$ and $P(z)$ by σ^{-3} and $\mu\sigma^{-3}$, respectively.

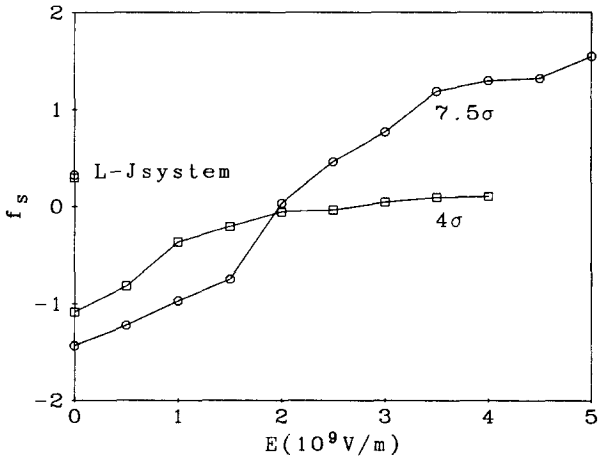

FIG. 2. The solvation force in units of ϵ/σ^3 for a Stockmayer fluid between plates separated by distances of $h = 4.0$ and $7.5\,\sigma$ as a function of the electric field **E**.

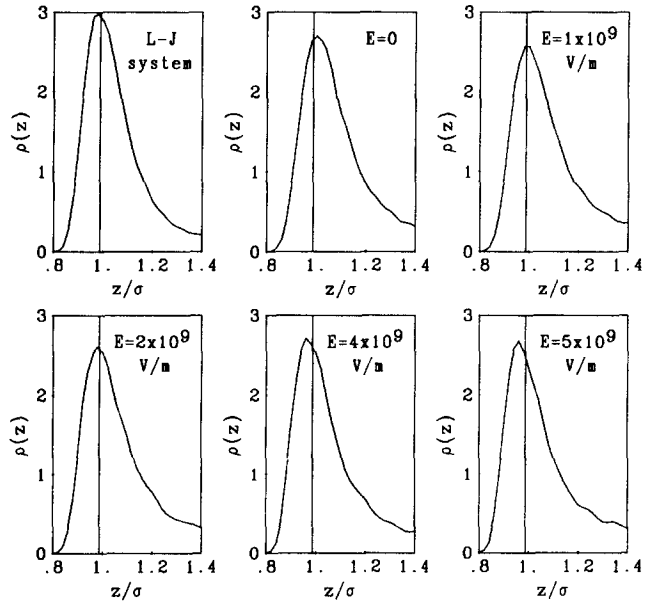

FIG. 3. The density profiles (near the left first layer) of Lennard-Jones and Stockmayer films with $h = 4.0\,\sigma$ when the field **E** ranges between 0 and 5×10^9 V/m. The vertical line is located at $z = 0.987\,\sigma$ where the wall–particle force is zero.

and translational motions. Periodic boundary conditions were applied in the x and y directions parallel to the walls using the minimum image convention. Also, the Ewald summations discussed earlier to take account of the long-ranged dipole–dipole interactions were performed in the x–y directions.[8,11] The computations were carried out in the microcanonical ensemble essentially as described by us in Ref. 1 starting with the equilibration of Lennard-Jones particles between Lennard-Jones walls followed by the introduction of point dipoles ($\mu = 1.36$ D) embedded in the particles and the application of an external electric field. Averages were computed after equilibration over several thousand time steps ranging from 10 000 to 30 000 except for the studies of monolayers when 250 000 time steps were used.

III. RESULTS AND DISCUSSION

In Fig. 1 the density and polarization density profiles of Stockmayer molecules with a field $\mathbf{E} = 10^9$ V/m between Lennard-Jones plates are plotted for various plate separations h. As pointed out for $h = 7.5\,\sigma$ in Ref. 1, the density profile for a Stockmayer fluid in the presence of an electric field is similar to the profile for a Lennard-Jones system[4,5] except for a slight decrease in the singlet density at the peaks adjacent to the walls and corresponding changes in the local density further away so that the area under these curves, which is equal to the number of particles in the system, is conserved.

In Fig. 2, the solvation force f_s on the plates is plotted as a function of the electric field **E** for $h = 4.0$ and $7.5\,\sigma$. The solvation force due to a Lennard-Jones fluid between two plates has been studied extensively by Snook and van Megan[4] and by Magda *et al.*[5] The addition of a dipole–dipole interaction to the Lennard-Jones molecules lowers the energy of the system as expected, and decreases the height of the first peak in the density profile near the walls. This is accompanied by a decrease in the solvation force between the plates, making it less repulsive (or more attractive) *at all of the plate separations studied by us.* However, it is evident

TABLE I. The solvation force in units of ϵ/σ^3 according to Eqs. (2.10a) and (2.10b) as a function of the plate separation h for Lennard-Jones or Stockmayer molecules between Lennard-Jones walls with and without an electric field $\mathbf{E} = 10^{10}$ V/m at 141 K. ($\epsilon = 119.8$ k, $\sigma = 3.405$ A, $\mu = 1.36$ D)

	LJ–LJ walls				Stockmayer fluid -LJ walls		Stockmayer fluid -charged LJ walls	
	Ref. 5		This work					
h/σ	(2.14a)	(2.14b)	(2.14a)	(2.14b)	(2.14a)	(2.14b)	(2.14a)	(2.14b)
2.25	−2.63	−2.63	−2.81	−2.79	−3.54	−3.52	−3.27	−3.29
2.5	−0.66	−0.66	−0.73	−0.74	−2.72	−2.73	−2.45	−2.45
2.75	4.92	4.92	4.86	4.85	2.72	2.72	3.15	3.14
3.0	0.49	···	0.36	0.37	−0.90	−0.90	−0.73	−0.73
3.2	−1.04	−1.05	−1.04	−1.05	−2.37	−2.36	−2.01	−2.02
3.5	0.0	0.01	−0.08	−0.08	−1.97	−1.97	−1.16	−1.16
3.75	1.65	1.65	1.52	1.52	−0.75	−0.75	−0.10	−0.10
4.0	0.38	···	0.33	0.32	−1.43	−1.43	−0.97	−0.97
7.5	0.22	0.26	0.31	0.28	−1.08	−1.09	−0.81	−0.81
9.5	0.18	0.19	0.23	0.22	−0.68	−0.68	−0.45	−0.46

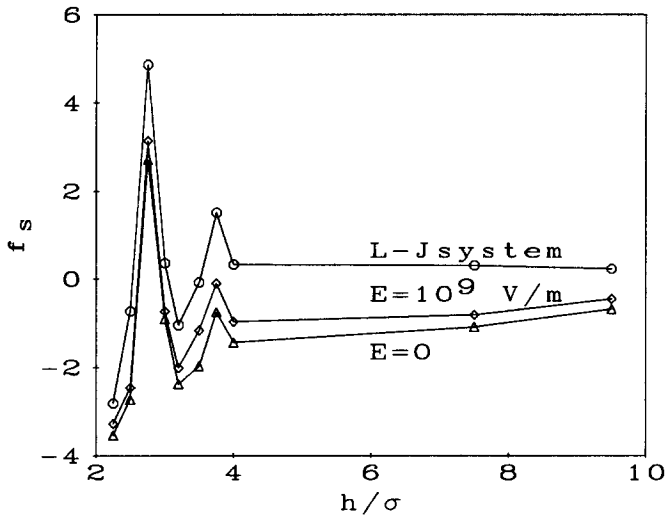

FIG. 4. The solvation force (units ϵ/σ^3) of Lennard-Jones (circles) and Stockmayer fluids without an electric field (triangles) and with a field $E = 10^9$ V/m (diamonds) between the plates as a function of the plate separation h.

from Fig. 2 that the solvation force on the plates increases when the electric field in the z direction is turned on. Although the field exerts no force on the molecules, it gives rise to a torque which tends to align the dipoles in the direction of the field, thereby leading to more pronounced layering of the fluid between the plates[1] and a shift of the first maximum in the density profile to positions closer to the walls as the field between the plates is increased (see Fig. 3). We find, from Eq. (2.10), that the minimum in the wall-particle potential lies at $z = 0.987\sigma$, and molecules located at positions $z < 0.987\sigma$ must therefore contribute to the repulsive part of the solvation force. An analysis of Fig. 3 shows that although the height of the first peak in the *density profile decreases slightly* as the field is applied, *the number of particles in the repulsive regions near the walls actually increases*, producing a solvation force that is more repulsive. Note that this force is not the total force acting between the plates when the field is turned on since this includes the direct electrical attraction between the plates which is independent of the nature of the fluid between them.

Table I contains additional details of the solvation force as a function of h when the electric field $E = 10^9$ V/m. This is calculated in two ways, from Eqs. (2.14a) and (2.14b), and the close agreement between the values obtained by these different routes confirms the accuracy of our computer simulations. A plot of the solvation force as a function of the plate separation h in Fig. 4 shows that it is an oscillatory function of h, even in the presence of a field, due to the segregation of particles into layers.[1] This was first suggested by the measurements of the solvation force of a nonpolar fluid by Horn and Israelachvili[11] and confirmed by computer simulation studies on Lennard-Jones fluids between plates by Snook and van Megan[4] and by Magda *et al.*[5] Our studies of these systems, which is the first step in our investigation of Stockmayer molecules between plates (see Sec. II), are in good agreement with these simulations. In Table II we provide details of the density profile $\langle \rho(z) \rangle$, the polarization density profile $\langle P_z(z) \rangle$, and the z component of the dipole moment $\langle \mu_z(z) \rangle$ for the system with a plate separation $h = 4.0\ \sigma$ at different values of the electric field. A similar

TABLE II. Molecular dynamics results of the local density $\langle \rho(z) \rangle$, the component of the dipole moment perpendicular to the wall $\langle \mu_z(z) \rangle$ and the polarization density $\langle P_z(z) \rangle$ for a Stockmayer fluid between Lennard-Jones walls separated by a distance $h = 4.0\sigma$ as a function of the electric field E across the plates.

E(10^9 V/m)	$\langle \rho(z) \rangle$		$\langle \mu_z(z) \rangle/\mu$	$\langle P_z(z) \rangle/\mu$	$\langle \rho(z) \rangle \langle \mu_z(z) \rangle/\mu$
0.0	1 st layers	2.7	0.0	0.0	0.0
	middle layer	1.5	0.0	0.0	0.0
0.5		2.7	0.15	0.42	0.41
		1.4	0.20	0.34	0.28
1.0		2.7	0.31	0.86	0.84
		1.4	0.31	0.58	0.43
1.5		2.6	0.46	1.26	1.20
		1.5	0.47	0.88	0.71
2.0		2.7	0.58	1.66	1.57
		1.5	0.55	1.03	0.83
2.5		2.7	0.69	1.93	1.86
		1.6	0.64	1.28	1.02
3.0		2.6	0.76	2.13	1.98
		1.5	0.68	1.31	1.02
3.5		2.7	0.81	2.27	2.19
		1.5	0.69	1.33	1.04
4.0		2.7	0.83	2.37	2.24
		1.5	0.71	1.36	1.07
4.5		2.7	0.85	2.45	2.30
		1.6	0.72	1.42	1.15
5.0		2.8	0.86	2.46	2.41
		1.6	0.74	1.45	1.18

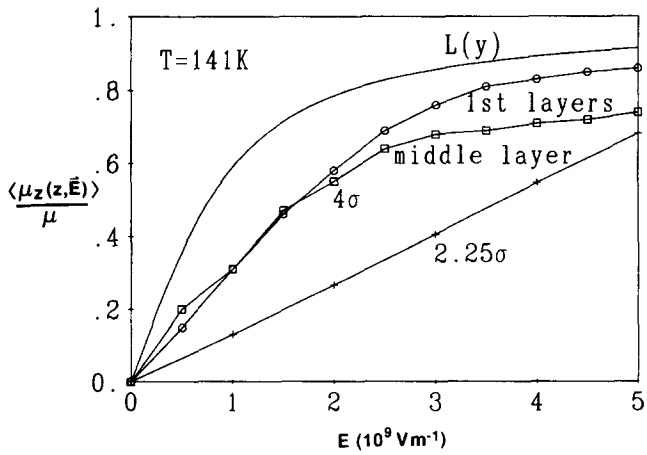

FIG. 5. The component of the dipole moment $\langle \mu_z(z) \rangle$ at 141 K in the direction of the electric field **E** as a function of **E** for plate separations of 4.0 σ (three layers) and 2.25 σ (monolayer).

study for a larger plate separation of $h = 7.5\,\sigma$ was discussed in our earlier paper[1] where it was found that the polarization density of each layer $\langle P_z(z,\mathbf{E}) \rangle = \langle \rho_z(z,\mathbf{E}) \mu_z(z,\mathbf{E}) \rangle$ was nearly equal to the product of $\langle \rho_z(z,\mathbf{E}) \rangle$ and $\langle \mu_z(z,\mathbf{E}) \rangle$, when the fluctuations in the numbers of particles in the layer were small. With $h = 4.0\,\sigma$ there are just three layers of particles (two outer layers next to the walls and a middle layer as shown in Fig. 1) between the plates, and the agreement with our approximation is found (see Table II) to be good, especially for the first layer. In Fig. 5 we plot $\langle \mu_z(z,\mathbf{E}) \rangle$ against **E** for this system ($h = 4.0\,\sigma$) and for the monolayer system ($h = 2.25\,\sigma$) and compare this with the Langevin function $L(y)$ with $y = (\mu|\mathbf{E}|/kT)$ which predicts values for $\langle \mu_z(z) \rangle$ that are too high. Note that for a monolayer $\langle \mu_z(z) \rangle$ appears to be a *linear* function of the electric field at 141 K for $\mathbf{E} < 5 \times 10^9$ V/m. Better agreement with the Langevin function is found[1] for thicker films ($h = 7.5\,\sigma$), from which it appears that this function is less accurate as an approximation for $\langle \mu_z(z) \rangle$ as the dimensionality changes from three to two.

The unusual behavior of the monolayer film was investigated further as a function of temperature and the electric field. Before discussing the dynamical properties of this system we present in Table III our calculations of the different terms which contribute to the total energy as a function of temperature and the electric field. Comparison may be made with the corresponding energy terms for a thicker film of dipoles ($h = 4.0\,\sigma$) in Table IV. The total energy for a Stockmayer fluid of mass m and moment of inertia **I** with dipole moment $\boldsymbol{\mu}$ between Lennard-Jones plates in the presence of the electric field **E** is

$$U = \sum_j 1/2\, m_i v_i^2 + (1/\mu^2) \sum_i 1/2\, \mathbf{I}\mu_i^2 - 1/2 \sum_{i \neq j} \sum_j \boldsymbol{\mu}_i \cdot \mathbf{T} \cdot \boldsymbol{\mu}_j + 1/2 \sum_i \sum_j U_{ij}^{\mathrm{LJ}} + \sum_i U_{w,i} - \sum_i \boldsymbol{\mu}_i \cdot \mathbf{E}. \quad (3.1)$$

The first two terms represent the translational and rotational kinetic energies, respectively, and the third, fourth, and fifth terms are the dipole–dipole, Lennard-Jones, and wall–particle interaction energies. The last term gives the energy of interaction between dipoles and the external electric field **E**. For a given electric field, the total energy of the sytem must be conserved since the simulation is carried out in the microcanonical ensemble. Table III and IV show how each energy term changes when the electric field $\mathbf{E} = 10^{10}$ V/m is turned on with plate separations of 2.25 σ and 4.0 σ. We see from the tables that, although there are significant changes in the dipole–field (DE) and dipole–dipole (DD) energies when the field is turned on, alignment of the dipoles with the field makes the DD interaction energy positive at $\mathbf{E} = 10^{10}$ V/m only for the monolayer system ($h = 2.25\ \sigma$) confined between two plates.

Snapshots of the particles in this layer at 141 K are shown in Figs. 6 at fields ranging from zero to 10^{10} V/m; the magnitude and length of the arrow drawn in each circle of radius $\sigma/2$ is proportional to the component of the dipole moment in the (x–y) plane parallel to the wall. The dipole autocorrelation functions are shown in Figs. 7 and 8. At zero field we have verified that the dipole autocorrelation function decays to zero at long times,[1] which is not the case at finite fields. Note that the polarization normal to the plates (z) increases and saturates as the field goes from 10^9 to 10^{10} V/m. Also note that the total dipole auto correlation function decays much faster at the highest field than at $\mathbf{E} = 0$ or 10^9 V/m. Apparently, the very slow relaxation of the transverse component at lower fields may be attributed to the dynamics of the loop/chain configurations discernible in Fig. 6. Figure 6 also shows that at 141 K, the dipoles, which

TABLE III. Thermodynamic results at $T = 141$ and 5 K for a monolayer film of Stockmayer molecules between Lennard-Jones walls separated by a distance $h = 2.25\sigma$, U_{LJ}, U_W, U_{DE}, U_{DD}, and U_{total} are the Lennard-Jones, particle–wall, particle–external field, dipole–dipole and total energies, respectively, while T_{trans}, T_{rot} are the translational and rotational temperatures in degrees Kelvin. All the energies are in reduced units of $N\epsilon$.

E(10^9 V/m)	$\langle U_{\mathrm{LJ}} \rangle$	$\langle U_W \rangle$	$\langle U_{DE} \rangle$	$\langle U_{DD} \rangle$	$\langle U_{\mathrm{total}} \rangle$	$\langle T_{\mathrm{trans}} \rangle$	$\langle T_{\mathrm{rot}} \rangle$
0.0	−1.45	−7.62	0.0	−6.95	−13.03	141.4	141.5
1.0	−1.49	−7.62	−0.45	−6.66	−13.23	141.3	141.8
10.0	−2.10	−6.93	−31.92	3.67	−37.84	141.3	141.5
0.0	−1.63	−7.87	0.0	−10.52	−19.82	5.0	5.1
1.0	−1.86	−7.86	−0.3	−10.25	−20.10	5.2	5.4
10.0	−2.52	−7.19	−33.87	3.87	−39.62	5.1	5.2

TABLE IV. Thermodynamic results at 141 K for the Stockmayer molecules between Lennard-Jones walls separated by a distance $h = 4.0\,\sigma$. The column headings and units are the same as in Table III.

E(10^9 V/m)	$\langle U_{LJ}\rangle$	$\langle U_W\rangle$	$\langle U_{DE}\rangle$	$\langle U_{DD}\rangle$	$\langle U_{total}\rangle$	$\langle T_{trans}\rangle$	$\langle T_{rot}\rangle$
0.0	− 3.27	− 3.23	0.0	− 6.96	− 10.50	141.7	141.5
10.0	− 3.58	− 3.10	− 32.70	− 2.69	− 39.11	141.8	141.8

are mainly oriented parallel to the walls in chains at zero field, are continuously transformed, with increasing electric field, into a state in which they are perpendicular to the walls at very high field. However, the pair distribution functions at 141 K (Fig. 9) do not show any compelling evidence of a transition to an ordered lattice even at the highest field 10^{10} V/m considered by us. As we shall see below, the system behaves differently at low temperature.

The snapshots of equilibrium configurations at zero field in Fig. 10 indicate an increase in chain length accompanied by the formation of close packed layers as the temperature is lowered. Comparison of the velocity auto correlation function (Figs. 11) at 141 and 5 K indicates tht the dipoles are vibrating about their equilibrium positions in the x–y plane at 5 K and that diffusion is negligible at this temperature. This suggests a phase transition below a critical temperature determined by the ratio of the energy of the dipoles at contact to the thermal energy as the relevant parameter.

In addition, an examination of the dipole autocorrelation functions (not shown) clearly indicates a frozen orientational configuration at 5 K with very small librational motion in the x–y plane.

In Fig. 12 we see how the equilibrium configurations of the dipoles in the monolayer are altered as the electric field between the plates is increased at 5 K. We are able to distinguish between three states (not necessarily separate phases), one of which is the chain-like structure observed in the absence of a field which has already been discussed. As the field is increased we next see a system of closely packed parallel chains of dipoles segregated into ferroelectric domains of opposite polarization. The orientation of dipoles in these domains is still largely perpendicular to the field [$\langle \mu_z(z)\rangle$ is relatively small] and adjacent layers of particles at the boundaries of the domains are displaced by half a molecular diameter thereby lowering the energy of the dipoles which are oriented in opposite directions at the boundaries. The density of this system is higher than the density at zero field, which suggests electrostriction. The pair correlation functions at zero field and a field of 10^9 V/m are qualitatively similar (Figs. 13) except for the appearance of an additional peak at 1.41 σ and satellite peaks at larger distances which

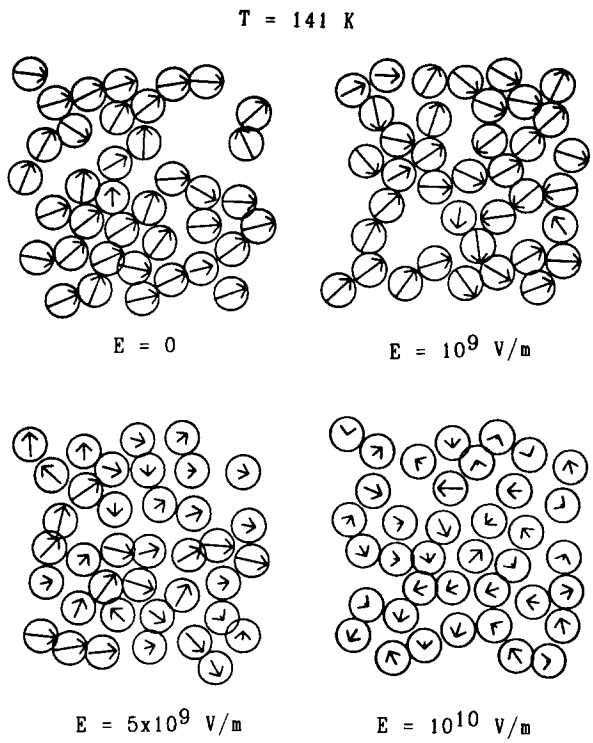

FIG. 6. Snapshots of a monolayer of Stockmayer dipoles between plates ($h = 2.25\,\sigma$) at 141 K and fields E ranging from 0 to 10^{10} V/m. The length of the arrow in each circle is proportional the component of the dipole moment parallel to the wall.

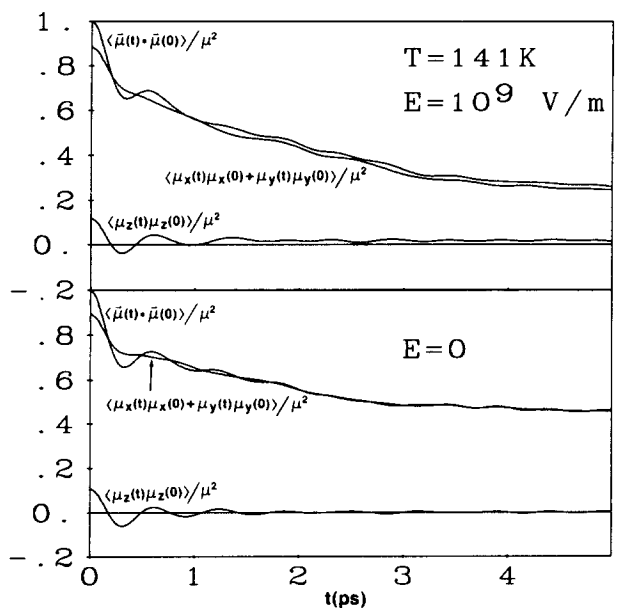

FIG. 7. The dipole auto correlation function of the Stockmayer monolayer at 141 K and E = 0 and 10^9 V/m. The components parallel and perpendicular to the wall are also shown.

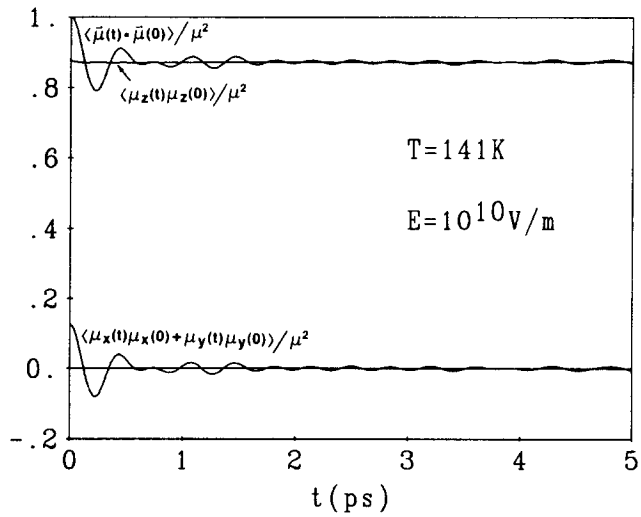

FIG. 8. The dipole autocorrelation functions of the monolayer dipolar system at 141 K when the field between the plates is 10^{10} V/m. The components parallel and perpendicular to the walls are also shown.

we ascribe to the correlations between particles in adjacent layers at the boundaries of the ferroelectric domains. A comparison (Fig. 14) of the velocity autocorrelation functions at 141 and 5 K at a field of 10^9 V/m suggests that decreasing temperature (see Fig. 12) is still the dominant factor in causing the particles to lose their diffusive motion and vibrate about their equilibrium positions at 5 K. A further increase in the field, however, leads to a pronounced alignment of the dipoles in the direction of the field and this gives rise to repulsion between dipoles and therefore a spatially less tightly bound configuration at 5 K. The reorientation of the dipoles parallel to the field is 100% complete at $\mathbf{E} = 10^{10}$ V/m (Fig. 15). Note that at 141 K $\langle \mu_z(z)\rangle/|\boldsymbol{\mu}|$ is 0.93 at this field. The velocity auto correlation function (Fig. 16) suggests that the particles have regained their diffusive motion. The diffusive motion of the particles is thus enhanced at the very highest fields when the particles are aligned with the field. This is true not only at 5 K but also at 141 K, as shown by the mean square displacement in the xy plane which is plotted as a

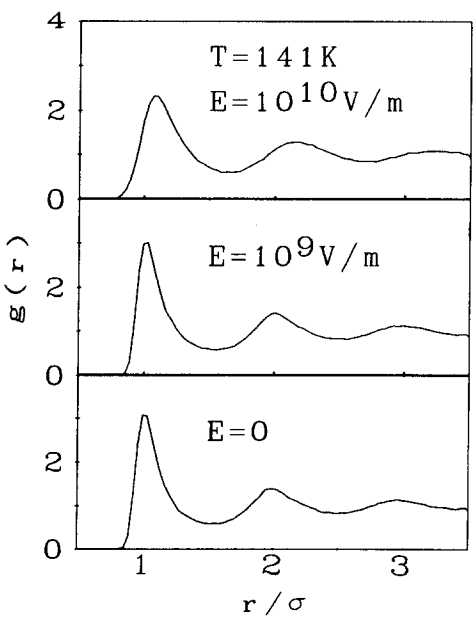

FIG. 9. Radial distribution functions of the monolayer of dipoles as shown in Fig. 6 at 141 K and several different values of the electric field.

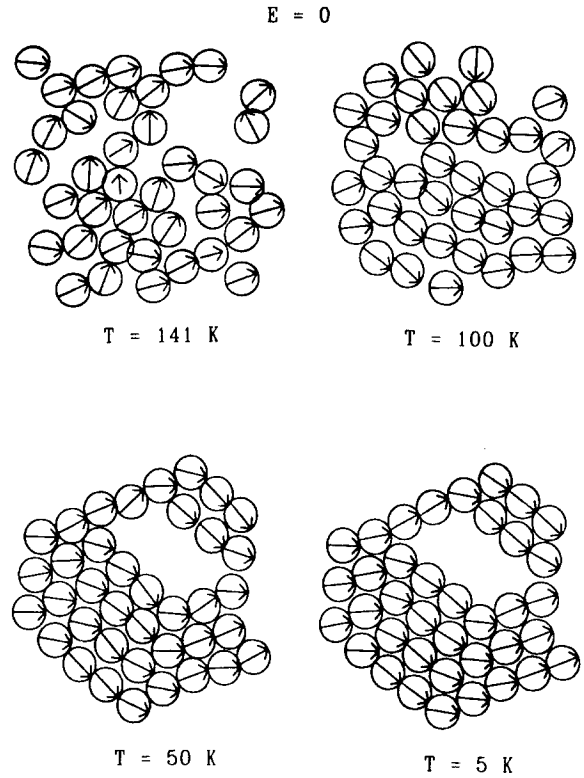

FIG. 10. Snapshots of a monolayer of Stockmayer dipoles between plates ($h = 2.25\,\sigma$) at zero field and temperatures ranging from 141 to 5 K. See the caption of Fig. 6 for other details.

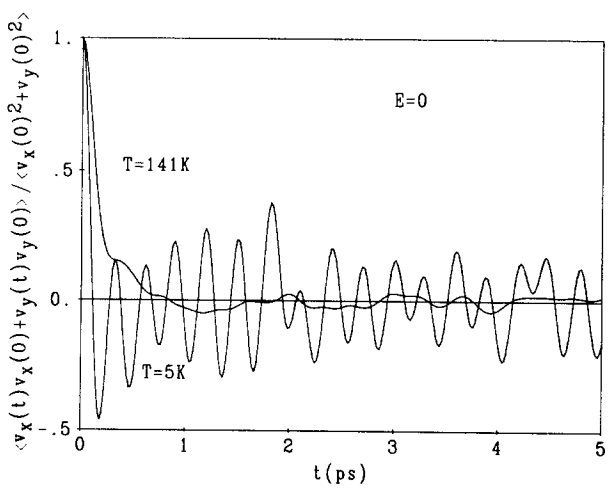

FIG. 11. The velocity autocorrelation functions of the molecules in a monolayer of a Stockmayer fluid between plates ($h = 2.25\,\sigma$) at 141 and 5 K and zero field.

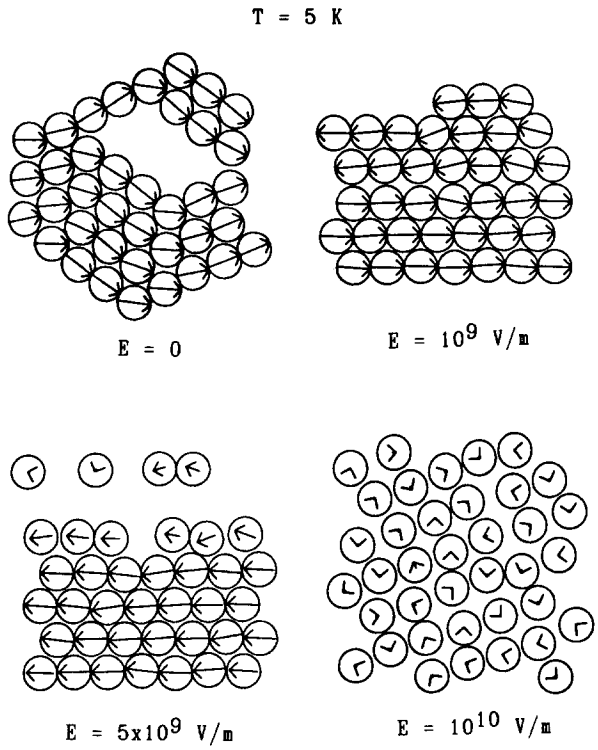

FIG. 12. Snapshots of a monolayer of Stockmayer dipoles between plates ($h = 2.25\,\sigma$) at 5 K and fields E ranging from 0 to 10^{10} V/m.

function of time in Fig. 17. Finally, the radial distribution function, $g(r)$ at 5 K, is shown in Figs. 18 when $\mathbf{E} = 10^{10}$ V/m. The structure observed (see Fig. 12) at 5 K suggests an imperfect (two-dimensional) triangular lattice.

Although our initial interest was in the behavior of a

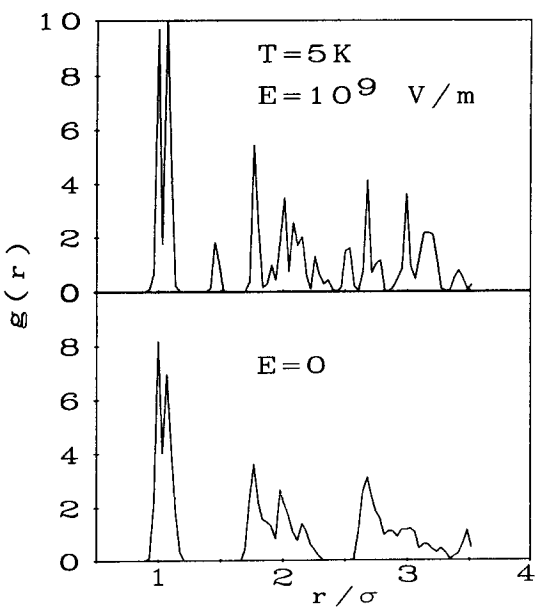

FIG. 13. Radial distribution functions for the Stockmayer fluid monolayer at 5 K and $\mathbf{E} = 0$ and 10^9 V/m.

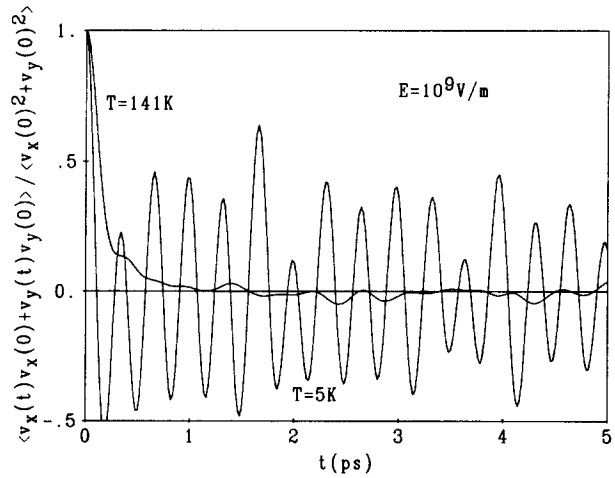

FIG. 14. The velocity autocorrelation functions of the molecules in a monolayer of a Stockmayer fluid between plates ($h = 2.25\,\sigma$) at 141 and 5 K and a field of 10^9 V/m. Figure 11 shows the correlation functions at zero field.

Stockmayer fluid between plates separated by several molecular diameters, our attention has become more focused on a dipolar monolayer in an external field over a range of temperatures. Though the equilibration time for such systems can be extremely long, it appears that meaningful simulations are well within the capability of modern computers. It now seems that a thorough MD investigation of the phase transitions in these systems is warranted.

While there exist an enormous literature on monolayers, detailed studies of dipolar fluid monolayers appear to be sparse. Phase diagrams of Langmuir monolayers of polar molecules were recently obtained analytically by Andelman, Brochard, and Joanny.[15] These authors used a Landau–Ginzburg expansion of the free energy to derive the near-critical behavior, while the low temperature structure was obtained via free energy minimization. In the case of dipoles oriented normal to the layer, the competition between long-range repulsive forces and short range van der Waals inter-

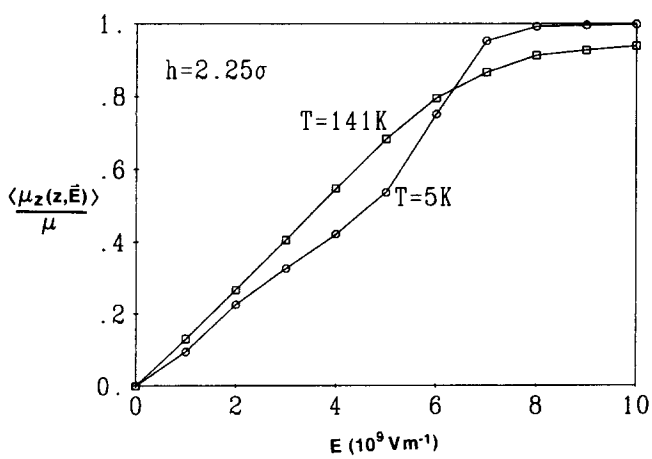

FIG. 15. The component of the dipole moment $\langle \mu_z(z) \rangle$ in the direction of the field as a function of the electric field E for the monolayer ($h = 2.25\,\sigma$) at 5 and 141 K.

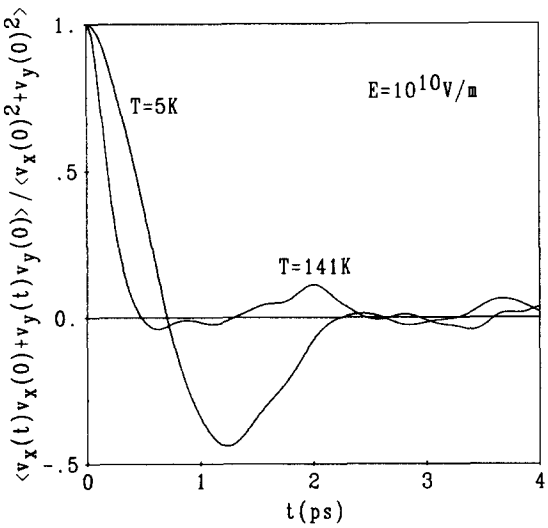

FIG. 16. The velocity autocorrelation functions of the molecules in a monolayer of a Stockmayer fluid between plates ($h = 2.25\,\sigma$) at 141 and 5 K and a field of 10^{10} V/m. Figures 11 and 14 show the correlation functions at zero field and a field of 10^9 V/m.

actions gives rise to novel phases in which the concentration is not uniform but rather has periodic (in-plane) oscillations. Also of relevance are the "interfacial colloidal crystal" melting transition studies by Kalia and Vashista,[16] Pieranski,[17] and Bedanov *et al.*[18] The MD simulation[16] indicates a first-order melting of the triangular lattice which occurs when the ratio of the average potential to kinetic energy falls below 60. A very similar transition occurs when a monolayer of micron-sized polystyrene spheres is suspended in a magnetic colloidal dispersion (ferrofluid) and subjected to a magnetic field applied normal to the layer.[19] The spheres acquire an apparent magnetic moment proportional to the external field, and the long range repulsive dipolar interactions induce a transition to a triangular lattice at some critical field. This system can be observed directly with a scanning electron microscope, and some striking photographs appear in Skjeltorp's papers.[19]

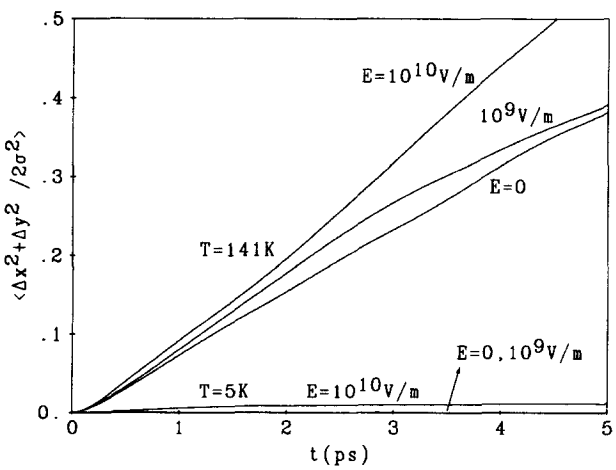

FIG. 17. The mean-square displacement of molecules parallel to the plates for a Stockmayer fluid when $h = 2.25\,\sigma$ at 141 and 5 K and fields $\mathbf{E} = 0$, 10^9, and 10^{10} V/m, respectively.

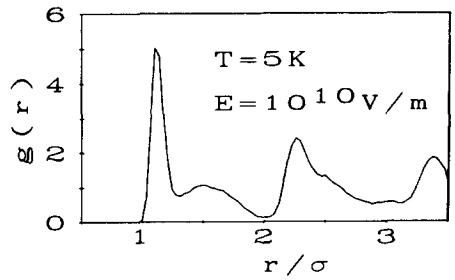

FIG. 18. Radial distribution function for the Stockmayer fluid monolayer at 5 K and a field of 10^{10} V/m.

ACKNOWLEDGMENTS

J.C.R. and S.H.L. would like to thank the National Bureau of Standards for computing facilities and hospitality during the period that this work was carried out. This research was supported by a grant to J.C.R. from the National Science Foundation (CHE-8305747).

APPENDIX: ROTATIONAL MOTION OF DIPOLES AND THE LEAPFROG ALGORITHM

The equation of motion [Eq. (2.17)] for the rotational degree of freedom of dipole i may be written as

$$\ddot{\boldsymbol{\mu}}_i(t) = a[\mathbf{R}_i(t) + 2\lambda_i \boldsymbol{\mu}_i(t)]\,, \tag{A1}$$

where $a = \mu^2/I$ and

$$\mathbf{R}_i(t) = \sum_{j \neq i} \mathbf{T}\cdot\boldsymbol{\mu}_j(t) + \mathbf{E}\,, \tag{A2}$$

in which $\mathbf{T}$ is the dipole interaction tensor [Eq. (2.2)] and $\mathbf{E}$ is the external field. The leapfrog algorithm[14] for this motion implies that

$$\dot{\boldsymbol{\mu}}_i(t + \Delta t/2) = \dot{\boldsymbol{\mu}}_i(t - \Delta t/2) + \Delta t \ddot{\boldsymbol{\mu}}_i(t) \tag{A3}$$

and

$$\boldsymbol{\mu}_i(t + \Delta t) = \boldsymbol{\mu}_i(t) + \Delta t \dot{\boldsymbol{\mu}}_i(t + \Delta t/2)\,. \tag{A4}$$

Combining Eqs. (A1), (A3), and (A4) we obtain

$$\boldsymbol{\mu}_i(t + \Delta t) = \boldsymbol{\mu}_i(t)[1 + 2a\lambda_i(\Delta t)^2] + \Delta t \dot{\boldsymbol{\mu}}_i(t - \Delta t/2) + a(\Delta t)^2 \mathbf{R}_i(t)\,. \tag{A5}$$

Applying the constraint

$$\boldsymbol{\mu}_i(t')\cdot\boldsymbol{\mu}_i(t') = \mu^2 \tag{A6}$$

to Eq. (A5) and taking $\Delta t = 1$ for convenience, leads to a quadratic equation for the Lagrangian multiplier λ_i

$$c_2 \lambda_i^2 + 2c_1\lambda_i + c_3 = 0\,, \tag{A7}$$

where

$$c_1 = 2a(\mu^2 + D + aG)\,, \tag{A8}$$

$$c_2 = 4a^2\mu^2\,, \tag{A9}$$

$$c_3 = B + Ca^2 + 2D + 2a(G + F)\,, \tag{A10}$$

and

$$B = \boldsymbol{\mu}_i(t - \Delta t/2)\cdot\boldsymbol{\mu}_i(t - \Delta t/2)\,, \tag{A11}$$

$$C = \mathbf{R}_i(t)\cdot\mathbf{R}_i(t)\,, \tag{A12}$$

$$D = \boldsymbol{\mu}_i(t)\cdot\dot{\boldsymbol{\mu}}_i(t - \Delta t/2)\,, \tag{A13}$$

$$F = \dot{\boldsymbol{\mu}}_i(t - \Delta t/2)\cdot\mathbf{R}_i(t)\,, \tag{A14}$$

$$G = \boldsymbol{\mu}_i(t)\cdot\mathbf{R}_i(t)\,. \tag{A15}$$

Taking the solution to Eq. (A7) with the positive sign in front of the square root, we have

$$\lambda_i = \left[-c_1 + (c_1^2 - c_2 c_3)^{1/2}\right]/c_2\,. \tag{A16}$$

[1]S. H. Lee, J. C. Rasaiah, and J. Hubbard, J. Chem. Phys. **85**, 5232 (1987).
[2](a) M. S. Wertheim, L. Blum, and D. Bratko, *Symposium on Colloidal Forces*, 189th meeting of the American Chemical Society, Miami, April 1985. (b) I. K. Snook and D. Henderson J. Chem. Phys. **68**, 2134 (1978).
[3]S. D. Sarma, K. E. Khor, S. M. Paik, and T. R. Kirkpatrick, Chem. Phys. Lett. **120**, 97 (1985).
[4]I. K. Snook and W. van Megen, J. Chem. Phys. **72**, 2907 (1980).
[5]J. J. Magda, M. Tirrell, and H. T. Davis, J. Chem. Phys. **83**, 188 (1985).
[6]G. Rickayzen in *Amorphous Solids and the Liquid State*, edited by N. H. March, R. A. Street, and M. Tosi (Plenum, New York, 1986), Chap. 6 and references therein.
[7]W. H. Stockmayer, J. Chem. Phys. **9**, 398, 863 (1941).
[8]D. J. Adams and I. R. McDonald, Mol. Phys. **32**, 931 (1976); V. W. Jansoone, Chem. Phys. **3**, 78 (1974); (S. W. de Leeuw, J. W. Perram, and E. R. Smith, Proc. R. Soc. Ser. A **373**, 57 (1980), and references therein.)
[9]L. V. Woodcock and K. Singer, Trans. Faraday Soc. **67**, 12 (1970).
[10]J. H. Irving and J. G. Kirkwood, J. Chem. Phys. **18**, 817 (1950).
[11]R. G. Horn and J. N. Israelachvili, J. Chem. Phys. **75**, 1400 (1981).
[12]J. P. Ryckaert, G. Ciccotti, and H. J. Berendsen, J. Comp. Phys. **23**, 327 (1977).
[13]E. L. Pollack and B. J. Alder, Physica, A **102**, 1 (1980).
[14](a) D. Potter, *Computational Physics* (Wiley, London, 1972); (b) R. W. Hockney, Methods Comput. Phys. **9**, 136 (1980).
[15]D. Andelman, F. Brochard, and J. F. Joanny (preprint).
[16]R. K. Kalia and P. Vashista, J. Phys. C **14**, L643 (1981).
[17]P. Pieranski, Phys. Rev. Lett. **45**, 569 (1980); P. Pieranski, L. Strzelecki, and B. Parser, Phys. Rev. Lett. **50**, 900 (1983).
[18]V. M. Bedenov, G. V. Gadiyak, and Yu. E. Lunyovik, Phys. Lett. A **92**, 400 (1982).
[19]A. T. Skjeltorp, J. Appl. Phys. **57**, 3285 (1985); J. Appl. Phys. **55**, 2587 (1984); Phys. Rev. Lett. **51**, 2306 (1983).